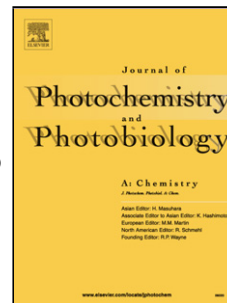


Journal Pre-proof

Effective Photodegradation of Organic Pollutants in the Presence of Mono and Bi-metallic complexes under Visible-Light Irradiation

Mahesh Subburu (Methodology) (Investigation) (Formal analysis) (Writing - original draft), Ramesh Gade, Venkanna Guguloth, Prabhakar Chetti, Koteswar Rao Ravulapelly, Someshwar Pola (Conceptualization) (Validation) (Formal analysis) (Resources) (Writing - review and editing) (Supervision) (Project administration)



PII: S1010-6030(20)30793-0

DOI: <https://doi.org/10.1016/j.jphotochem.2020.112996>

Reference: JPC 112996

To appear in: *Journal of Photochemistry & Photobiology, A: Chemistry*

Received Date: 1 June 2020

Revised Date: 19 October 2020

Accepted Date: 22 October 2020

Please cite this article as: Subburu M, Gade R, Guguloth V, Chetti P, Ravulapelly KR, Pola S, Effective Photodegradation of Organic Pollutants in the Presence of Mono and Bi-metallic complexes under Visible-Light Irradiation, *Journal of Photochemistry and Photobiology, A: Chemistry* (2020), doi: <https://doi.org/10.1016/j.jphotochem.2020.112996>

This is a PDF file of an article that has undergone enhancements after acceptance, such as the addition of a cover page and metadata, and formatting for readability, but it is not yet the definitive version of record. This version will undergo additional copyediting, typesetting and review before it is published in its final form, but we are providing this version to give early visibility of the article. Please note that, during the production process, errors may be discovered which could affect the content, and all legal disclaimers that apply to the journal pertain.

© 2020 Published by Elsevier.

Effective Photodegradation of Organic Pollutants in the Presence of Mono and Bi-metallic complexes under Visible-Light Irradiation

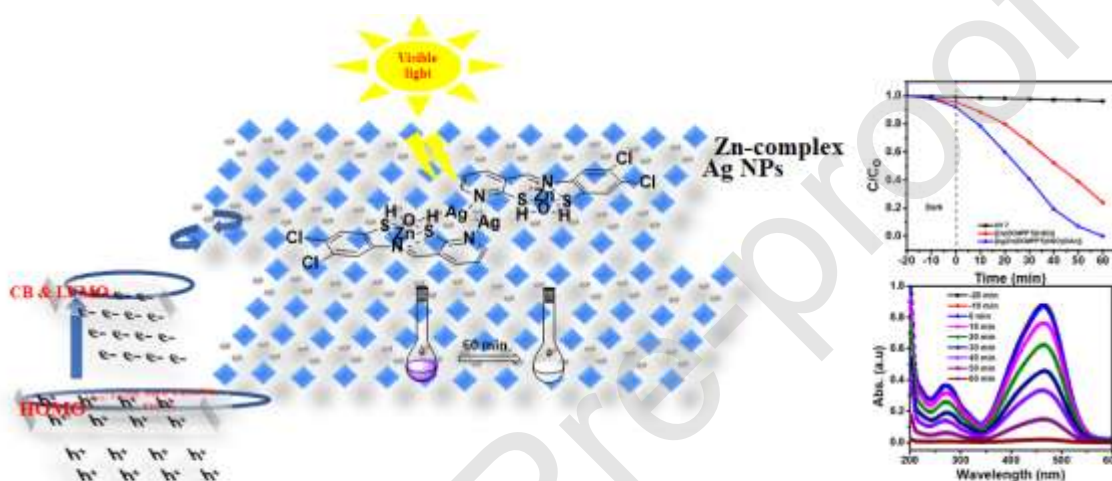
Mahesh Subburu,^a Ramesh Gade,^a Venkanna Guguloth,^a Prabhakar Chetti,^b Koteswar Rao Ravulapelly,^a and Someshwar Pola^{a*}

^aDepartment of Chemistry, Osmania University, Hyderabad, India.

^bDepartment of Chemistry, National Institute of Technology, Kurukshetra, India.

*Corresponding author: E-mail address: somesh.pola@gmail.com Tel: + 919959972288

Graphical Abstract



[Ag-Zn(DCMPPT)(H₂O)(OAc)] complex act as photocatalyst for degradation of organic dye pollutants and industrial wastewater under visible light irradiation due to Ag nanoparticles are insitu generation from bi-metallic complex then which helps to holes stability in HOMO of complex.

Highlights

- Synthesis of new Zn (II) complex and Ag-Zn bi-metallic complex using organic functional group-based ligand which consists of N and S donor atoms for complexation.
- Several spectroscopic techniques are used for characterization new complexes.

- New complexes act as photocatalysts for degradation of organic dye pollutants and industrial wastewater under visible light irradiation.
- Identification of active species for the degradation of degradation of organic dye pollutants and industrial wastewater is hydroxy radicals from scavengers study.

Abstract

The synthesis of new mono and bi-metallic complexes such as Zn (II) and Ag-Zn (II) complexes with organic functional group-based ligand (OFL) presented in the current work along with the exploration of their applicability in the photocatalytic degradation of organic dyes under visible-light irradiation. The Zn (II) complex obtained from organic functional group-based ligands, complexed with the donor atoms such as S and N under solvothermal conditions and Ag-Zn (II) complex formed through Ag ions complexed with pyridine ring nitrogen atom. These Zn(II)-complexes were systematically analyzed using the physicochemical studies and other spectroscopic techniques. From these facts, it is clarified that the complexes show square planar geometry with organic functional group-based ligands coordination *via* mercapto and azomethine groups. The reported complexes were used for the photodegradation of standard organic dye pollutants used in various textile and food processing industries. The complex [Ag-Zn(DCMPPT)(H₂O)(OAc)] shows higher photocatalytic activity than [Zn(DCMPPT)(H₂O)] because of the high surface area, low bandgap energy and further visible-light available for the initiation of •OH radicals. To identify the active species in the photocatalytic process, the mechanism process also reported for the fast photodegradation of organic dye pollutants in the existence of some radical quenchers.

Keywords: Ag(I)-Zn(II) bi-metallic complex, Ag nanoparticles, Wastewater, Photodegradation

Introduction

Most of the organic dye pollutants are toxic and produce very serious ecological pollution by discharging harmful materials into the marine system and are not easy to degrade in water. Purification of industrial wastewater is a big task or mission for environmental scientists to regulate a few kinds of chemicals by several procedures such as physico-chemical, microbial, and photodegradation methods [1-3]. Still, these methods are not reached the purposeful

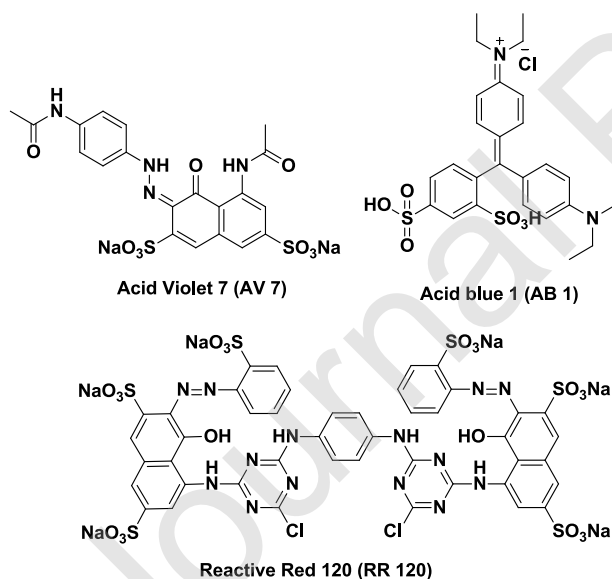
investigation for the removal of toxic pollutants and the processes are also very expensive. To this observation, enormous research efforts have been made on the photodegradation of industrial wastewater using pure semiconductor oxides. Semiconductor oxides show photodegradation of organic pollutants due to their high stability, non-toxicity, but these are also having high manufacturing cost [4]. However, semiconductor oxides show lower catalytic performance because of the large bandgap energy, the particles size is not equal and very high recombination energy [5]. Another new technique is an advanced oxidation process (AOPs) [6-8], which is one of the paths to produce $\bullet\text{OH}$, but it is also a highly expensive method.

OFLs based metal complexes are an important class of molecules due to different oxidation states, monitoring the fulfillment of metals in an enormous diversity of suitable catalytic conversions. Meanwhile, in the last few decades, magnetic properties, structural arrangements and spectroscopic information of Schiff's base complexes have been examined [9-11]. The metal complexes of the OFLs receiving a widerange of applications such as photocatalytic, analytical, biological and industrial due to their significant performance in catalysis for new organic transformations [12-16]. The metal complex of OFLs also acts as photocatalysts for photodegradation of organic pollutants [17]. Hence, OFL ligand-based metal complexes are crucial for the photocatalytic degradation of organic dye pollutants under visible light conditions.

Recently, photodegradation of organic dye pollutants by using Ti (IV) Schiff's base complexes have been reported for the degradation of methylene blue [18] and also reported Ag-dopedPd(II) complex for degradation of azo-dyes under visible light irradiation [19]. Kadiiska and co-workers described that a series of radical ions or radicals with $\text{HO}_2\bullet/\text{O}_2\bullet^-$ and $\bullet\text{OH}$ were stimulated in the photocatalytic process [20]. Further, Singh et al. described that [Fe(III)-salen]Cl complex has been used for the degradation of organic-dye contaminants [21]. It is observed from the literature that in several numbers of photodegradation methods, hydrogen peroxide (H_2O_2) is playing a significant role in the generation of highly active radical species such as $\bullet\text{OH}$ radicals and is reacts with toxic molecules for the photomineralization method [21]. However, usage of a larger quantity of H_2O_2 is unsafe and affectsthe health conditions of humans. Recently, some types of Ni(II)-complexes obtained from Schiff's bases were utilized for the degradation of rhodamine-B (RhB) and methylene blue (MB) dyes without using of H_2O_2 , as photocatalysts used under visible-light conditions [16,22]. The zeolite captured Ni(II) and Cu(II) Schiff's base

complexes used for oxidation of benzhydrol and photodegradation of RhB dye under visible-light and time taken for degradation was 3 to 4 hours [23]. The majority of the studies on Schiff's base metal complexes are pH-sensitive, if the pH of the solution is greater than 9, the metal complexes are less stable [24]. Also, most of the known metal-organic frameworks act as photocatalysts are not having much variation in the structures and their structure-activity relationship and it is still unclear [25].

Metal complexes used for several organic transformations [26], but there are few gaps found in the field of photocatalysis like degradation of organic dye pollutants. For this reason, OFL based complexes are focused on the development of visible light sensitive photocatalysts with some significant features such as photostability, less recombination energy, high surface area, recyclable, and reasonable synthetic methodology. Photocatalysts are using OFL based complexes underneath visiblelight has motivating significant consideration due to its prospective properties in biodegradable remediation by parting the organic dye pollutants to very harmless products.



Scheme 1 Structures of various dyes used for photodegradation

In one such study, the new Schiff's base Zn(II) and Ag-Zn(II) complex synthesis from N, S-donor based tridentate OFLs are reported. The newly synthesized $[Zn(DCMPPT)H_2O]$ and

[Ag-Zn(DCMPPT)(H₂O)(OAc)] complexes are used for photodegradation of selected organic dye toxic molecules under visiblelight irradiation (selected organic dyes are shown in Scheme 1).

EXPERIMENTAL SECTION

Materials and Methods

All starting materials purchased from Alfa Aesar and listed as Ag(OAc), Zn(OAc)₂, various dyes, phenylglyoxylic acid, ammonium tetrathiocyanodiammonochromate (Reinecke salt from Sigma-Aldrich) directly used for complexation and photodegradation process. Preparation of organic functional ligand (E)-3-(((4,5-dichloro-2-mercaptophenyl)imino)methyl)pyridine-2-thiol (DCMPPT)'' was carried out as per earlier reported method [18].

Synthesis of complexes

Preparation of the Zn((E)-3-(((4,5-dichloro-2-mercaptophenyl)imino)methyl)pyridine-2-thiol) [Zn(DCMPPT)(H₂O)]

A 20 ml ethanol solution of DCMPPT ligand (1.00 mmol) and one equivalent amount of Zn(OAc)₂ was added in the reaction flask with continuous stirring at room temperature conditions for 30 min. and shown in Scheme 2. The reaction mass was refluxed for a further four hours at 80 - 90°C. Then the reaction mixture cooled to room temperature, the precipitated complex product was filtered to get solid crude complex. The obtained crude product was washed with various solvents such as acetone, methanol, and diethyl ether to obtain pure pale-yellow compound with a 74% yield.

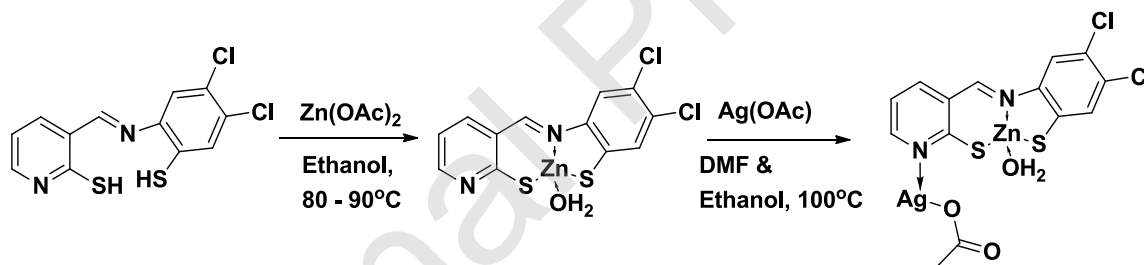
R_f 0.28 (9:1 ratio of CHCl₃/MeOH); Molecular formulae: C₁₂H₈Cl₂N₂OS₂Zn; CHN analysis expt. (calcd): C% 36.29 (36.34), H% 2.01 (2.03), Cl% 17.84 (17.88), N% 7.01 (7.06), S% 16.14 (16.17) and Zn% 16.43 (16.43); ¹H NMR (400MHz, *d*₆-DMSO) δ (ppm) = 8.28 (m, 1H), 7.82 (m, 1H), 7.62 (s, 1H), 7.48(m, 1H), 7.13 (s, 1H), 6.92 (s, 1H) and 3.52 (br, 2H); ¹³C NMR (100 MHz CDCl₃) δ (ppm) = 162.842, 147.305, 143.242, 142.842, 139.197, 132.008, 130.875, 130.528, 130.446, 129.725, 128.403, 127.671, 127.574, 126.868, 125.890, 113.744, and 109.790; MS (EI): 375.8639 (M-(H₂O))⁺; UV-Vis: 291.12, and 405.02 nm.

Preparation of the bi-metallic complex [Ag-Zn((E)-3-(((4,5-dichloro-2-mercaptophenyl)imino)methyl)pyridine-2-thiol)(H₂O)(OAc)]([Ag-Zn(DCMPPT)(H₂O))(OAc)]:

Silver acetate (1.00 mmol) was placed in 10 ml solution of [Zn(DCMPPT)(H₂O)] (1.00 mmol, in DMF and ethanol (2:8)) with continuous stirring at ambient conditions. Then the

reaction mixture was heated for four hours and continued for a further one hour at 100°C (Scheme 2). After five hours, the reaction mixture cooled to room temperature to get a dark-colored crude product. The crude material was filtered and washed with double distilled water, acetone, cold methanol, and diethyl ether to find pure dark-grey with shiny solid [Ag-Zn(DCMPPT)(H₂O)(OAc)] material with 48 % yield. Furthermore, to check the complexation of Ag ions in the complex formation process, the rest of the solution was titrated with 0.1 M KCl solution ensuing no formation of a solid precipitate of AgCl, this shows a calculable quantity of Ag complexed and obtained pure bi-metallic complex.

R_f 0.22 (8:2 ratio of CHCl₃/MeOH); Molecular formulae: C₁₅H₁₃AgCl₂N₂O₃S₂Zn; CHN analysis expt. (calcd): C% 31.15 (31.19), H% 2.24 (2.27), Cl% 12.24 (12.28), N% 4.83 (4.85), Ag% 18.64 (18.68), S% 11.07 (11.10) and Zn% 11.26 (11.32); ¹H NMR (400MHz, d₆-DMSO) δ (ppm) = 8.23 (m, 1H), 7.83 (m, 1H), 7.59 (s, 1H), 7.48 (m, 1H), 7.18 (s, 1H), 6.92 (s, 1H), 3.68 (br, 2H), and 2.36 (s, 3H); ¹³C NMR (100 MHz CDCl₃) δ (ppm) = 204.933, 166.859, 140.860, 138.328, 130.695, 130.353, 130.207, 130.148, 129.522, 129.215, 129.070, 128.989, 128.931, 128.873, 128.822, 128.654, 128.267, 127.953, 127.838, 127.422, 127.262, 126.859 and 26.859; MS (ED): 560.7929 (M+1)⁺; UV-Vis: 293.46 and 408.06 nm.



Scheme 2 Synthesis of new [Zn(DCMPPT)(H₂O)] and [Ag-Zn(DCMPPT)(H₂O)](OAc) complexes

Estimation of surface area

BET surface areas were determined by N₂ adsorption at liquid nitrogen temperature using a BELSORP-mini II instrument (BEL JAPAN, INC.). Prior to the measurement, the samples were degassed at 200 °C for 2 h.

Photodegradation reactions

Photodegradation of various organic dyes

The photocatalyst (25 mg) was added to a dye pollutant 50 mL solution (5 × 10⁻⁵ M) in an 80 mL quartz glass cylinder type tubular photoreactor. The degradation of various the dyes was

kept in the occurrence of visible-light (50 Watts LED light with photon flux is 8.92×10^{13} Einstein/s and wavelength 380-840 nm), as observed by using the chemical actinometric technique with Reinecke salt [5] for 60 min. Adsorption-desorption equilibrium procedure for the individual dye was achieved in the absence of light for 20 min then the light is allowed to fall on the reaction mixture. Once the light is turned on then each 10 min of time interval sample was taken for analysis, photocatalyst was separated by filtration and examined using a UV-visible spectrophotometer at dye λ_{\max} .

Photodegradation of Industrial Wastewater (IWW)

The photocatalyst (complexes) (50 mg) was dispersed in 200 mL of industrial wastewater (IWW) in a 500 mL cylindrical quartz glass reactor. The photodegradation of IWW was carried out under visible light (50 Watts LED light) for 240 min. Adsorption-desorption pre-equilibrium of the dye was attained in the dark for 60 min. before irradiation and sampling. Samples were collected every 30 min. for analysis and filtered through a Millipore filter (MF-Millipore Membrane Filter, 0.22 μm pore size) to remove the catalyst particles and then examined by UV-Vis spectrophotometer at respective λ_{\max} value.

Controlled photoreaction for identification of in-situ formed Ag NPs

The photocatalyst (50 mg) was dispersed in 50 mL of double distilled water in an 80 mL cylindrical quartz glass reactor. The photoreaction of water was carried out under visible light (400 Watts Tungsten light) for 60 min. For every 10 min of time samples were collected for analysis and filtered through a Millipore filter (MF-Millipore Membrane Filter, 0.22 μm pore size) to remove the catalyst particles and then examined by UV-Vis spectrophotometer at respective λ_{\max} value.

Results and Discussion

Methods used for the characterization of complexes with various spectroscopic techniques and their details are described in the supplementary information.

Characterization of photocatalysts

The Zn (II) and bi-metallic complexes are non-hydroscopic and are very stable at ambient conditions. Complexes are completely soluble in DMF, and DMSO, but very less soluble in acetone, chloroform, methanol and ethanol. The EDX information of both complexes is revealed in **Figure 1**. The EDX spectrum shows that Ag, Zn, S, N, Cl, and O atoms are existing in the

complex. Which designated that the Zn^{2+} ions are complexed to tridentate ligand unit and Ag^+ also complexed through pyridine rings.

Mass Spectral data, molar conductance and FESEM morphological studies

The mass spectral data of complexes reveals that the base peaks are matching with $[Zn(DCMPPT)]^+$ and $[Ag-Zn(DCMPPT)H_2O(OAc)]$ [19] (Figure S1 and S2). In mass spectra of $[Zn(DCMPPT)(H_2O)]$, showed two peaks with two different m/z values such as 394.8751 and 376.8648 respectively. These peaks indicated that $[M+1]^+$ molecular ion and $[(M+1)-H_2O]^+$ fragmented ion peak respectively. Similarly, in the case of $[Ag-Zn(DCMPPT)(H_2O)(OAc)]$ complex exhibited that three significant peaks with m/z values such as 560.7934 ($[M+1]^+$), 501.7801 ($[M+1]-OAc)^+$ and 376.8647 ($[(M+1)-OAc-(Ag^+H_2O)]^+$) ions respectively.

Ionic or covalent nature of the new Zn(II) complexes identified through molar conductance studies. The low molar conductance values revealed that both the complexes in DMF solvent indicated that these complexes are covalent due to the presence of water molecule and acetate ions in inside the coordination sphere ($[Zn(DCMPPT)H_2O]$ and $[Ag-Zn(DCMPPT)H_2O(OAc)]$ [18,27] and the corresponding data presented Table 1. The morphological studies of Zn(II) complexes have completely reformed in its shape and size when associated with the ligand DCMPPT compared to the morphology of ligand alone. The FESEM imageries of Zn(II) complexes exhibited that the particles form nanoflakes, subsequently re-complexed with Ag ions and the total morphology transformed into nanocubes [28]. Comparison of nanosheet type $[Zn(DCMPPT)(H_2O)]$ with ligands is shown in **Figure 2**.

Table 1. Physico-chemical, % of elements and molar conductivity data of ligand and complexes

Compound	% Yield	^a M.P/D. P. (°C)	%C (calcd)	%H (calcd)	%Cl (calcd)	%N (calcd)	%S (calcd)	%M (calcd)	$\Lambda_m \text{ ohm}^{-1} \text{ mol}^{-1} \text{ cm}^2$ (DMF)
*L	78	186	45.68 (45.72)	2.54 (2.56)	22.51 (22.49)	8.85 (8.89)	20.31 (20.34)	--	---
$C_{12}H_8Cl_2N_2S_2$ $[Zn(L)H_2O]$	74	254	36.31 (36.34)	2.02 (2.03)	17.85 (17.88)	6.99 (7.02)	16.15 (16.17)	16.46 (16.48)	10.68
$C_{12}H_8Cl_2N_2OS_2Zn$ $[Ag-Zn(L)H_2O](OAc)$	48	306	29.79 (29.84)	1.95 (1.97)	12.54 (12.58)	4.94 (4.97)	11.34 (11.38)	19.12 (19.14)	14.78
$C_{14}H_{11}AgCl_2N_2O_3S_2Zn$								11.58 (11.60)	
								(Zn)	

*L = DCMPPT

Thermogravimetric and XPS studies

The thermograms (**Figure 3**) of the Zn (II) complexes exhibit two stages percentage weightloss, significant in the temperature range of 200 – 450 °C which indicates that coordinated water molecules and ligand part. Therefore, two-step decomposition specified that complexes are associated with one water and ligand molecule and formed square planar complexes[29-31]. The obtained residues were examined by using XPS. The data found that the binding energies of various elements present in residues are N, O, S and Zn in [Zn(DCMPPT)(H₂O)] and Ag, N, O, S and Zn in [Ag-Zn(DCMPPT)(H₂O)(OAc)] respectively, and are shown in **Figure 4**.

Powder XRD (P-XRD) pattern of ligand and complexes

The P-XRD peaks of the DCMPPT OFL exhibited 2θ values that exist in between 5 and 50 with high-intensity 2θ peak at 5.82°(111). Nevertheless, [Zn(DCMPPT)(H₂O)] complex peaks were altered when related to the DCMPPT. Hence, Zn²⁺ ion has been complexed with the N, and S donor atoms and H₂O molecule of the OFL. A peak showed in DCMPPT at 2θ = 9.68°(111) was increased after coordination with Zn²⁺ ions, and one more maximum peaks at 2θ = 21.53° (100) and 25.09° (220) was shifted to higher 2θ value side. Also, in the bi-metallic complex, all the peaks shifted to higher 2θ value side which designated that the development of a characteristic Ag-Zn based framework, especially a broad peak around 2θ = 25.12° (220), recognized to the interlayer distance in [Ag-Zn(DCMPPT)(H₂O)(OAc)]. In the complexes, two sulphur and one N-atoms and one water molecule are coordinated with Zn and geometrically arranged as square planar complex and Ag nanoparticles are occupied in between two Zn-complexes and form a layered type MOFs with acetate ions placed inside the coordination sphere. All the peaks were broadened and a reference peak was shown at 44° (200) [32], which indicated that presence Ag ions in between the layers of the [Zn(DCMPPT)(H₂O)] complex as shown **Figure 5**. The unit cell parameters of DCMPPT, [Zn(DCMPPT)(H₂O)], and [Ag-Zn(DCMPPT)(H₂O)(OAc)] materials are obtained by least-square fitting using **POWD** software. The unit cell parameters of DCMPPT, [Zn(DCMPPT)(H₂O)], and [Ag-Zn(DCMPPT)(H₂O)(OAc)] (DCMPPT: monoclinic lattice, a = 10.432 Å, b = 4.912 Å, c = 9.452 Å, and β = 103.64°, *P21/c* space group; [Zn(DCMPPT)(H₂O)]: orthorhombic lattice, a = 9.517 Å, b = 13.412 Å, c = 33.140 Å, and α = β = γ = 90°, *Pna2(1)* space group; [Ag-Zn(DCMPPT)(H₂O)(OAc)]: triclinic lattice, a = 13.823 Å, b = 14.283 Å, c = 14.453 Å, and α = 82.55°, β = 78.34°, γ = 72.69°, *P1* space group) are given as input parameters for least-square

fitting the powder data of DCMPPPT, $[\text{Zn}(\text{DCMPPT})(\text{H}_2\text{O})]$, and $[\text{Ag-Zn}(\text{DCMPPT})(\text{H}_2\text{O})(\text{OAc})]$ materials [33-36].

IR and NMR studies

The IR bands of Zn and bi-metallic complexes provide a shred of evidence about the coordination with Zn^{2+} ions with ligand and also, Ag^+ ions re-complexed with Zn-complex. All the peaks of complexes are compared with ligands and are shifted its wavenumber by 15- 25 cm^{-1} due to complexation between Zn and ligand through azomethine and -SH groups [18]. Some new peaks were also found at 860, 432, and 387 cm^{-1} , which belongs to the coordinated water molecule, and $\nu(\text{Zn-S})$ and $\nu(\text{Zn-N})$ of azomethine groups respectively, and are shown in Figure S3. $^1\text{H-NMR}$ spectra of complexes such as $[\text{Zn}(\text{DCMPPT})(\text{H}_2\text{O})]$ and $[\text{Ag-Zn}(\text{DCMPPT})(\text{H}_2\text{O})(\text{OAc})]$ were analyzed in d_6 -DMSO and CDCl_3 . The significant peaks of ligand were disappeared as compared to complex spectra and azomethine proton was deshielded, and also attached aromatic hydrogen atoms are slightly deshielded, which indicated that Zn (II) complex was formed through N, S donor atoms of ligand [37]. However, one more important broad peak at 3.58 ppm was also observed, which belongs to the coordinated water molecule of the $[\text{Zn}(\text{DCMPPT})(\text{H}_2\text{O})]$ complex. Whereas, in case of $[\text{Ag-Zn}(\text{DCMPPT})(\text{H}_2\text{O})(\text{OAc})]$ complex, spectrum presented some significant variations compared with the $[\text{Zn}(\text{DCMPPT})(\text{H}_2\text{O})]$ complex, a new peak at 2.36 ppm of acetyl group protons with a singlet and aromatic protons are moved to the up-field side as revealed in Figure S4 and S5. Hence, it is specified that Ag ions existing and coordinated with pyridine ring N atom, in $[\text{Ag-Zn}(\text{DCMPPT})(\text{H}_2\text{O})(\text{OAc})]$ complex. Also, in $^{13}\text{C-NMR}$ spectra of the $[\text{Zn}(\text{DCMPPT})(\text{H}_2\text{O})]$ peaks were changed compared with the DCMPPPT ligand spectrum (Figure S6 and S7). Hence, complexes are extremely stable and Zn (II) ions are fit into tridentate ligand and complexing through N and S atoms of the ligand. Finally, established on bases of spectral data the $[\text{Zn}(\text{DCMPPT})(\text{H}_2\text{O})]$ and $[\text{Ag-Zn}(\text{DCMPPT})(\text{H}_2\text{O})(\text{OAc})]$ complexes are coordinated through S and N atoms and as shown in **Figure 6**.

Electronic spectral and surface area studies

The electronic properties of the $[\text{Zn}(\text{DCMPPT})(\text{H}_2\text{O})]$ and $[\text{Ag-Zn}(\text{DCMPPT})(\text{H}_2\text{O})(\text{OAc})]$ in DMF were examined. **Figure 7a** reveals the UV-vis spectra of the $[\text{Zn}(\text{DCMPPT})(\text{H}_2\text{O})]$ and $[\text{Ag-Zn}(\text{DCMPPT})(\text{H}_2\text{O})(\text{OAc})]$ in solution. The Zn(II) complexes show a significant band, and this band is spin-allowed transition due to squareplanar geometry

and the bands assigned as $T_{2g} \rightarrow T_{1u}$ [38]. From absorption spectra, the bandgap values are estimated from the onset λ value of spectra. A strengthening of the UV-Vis Light Diffuse Reflectance spectra of DCMPT, [Zn(DCMPPT)(H₂O)] and [Ag-Zn(DCMPPT)(H₂O)(OAc)] samples described in **Figure 7b**, it reveals that the existence of an extensive surface plasmonic resonance (SPR) band between 340 and 550 nm well-matched to the SPR of Ag ions and are complexed with [Zn(DCMPPT)(H₂O)]. The bandgap energy values attained from UV-vis-DRS solid state are shown in Table 2.

From the UV-vis-DRS spectra OFL and Zn-complexes bandgap values (E_g) are evaluated by using the Kubelka-Munk method using the following equations 1 and 2 [39]:

$$F(R) = \frac{(1-R)^2}{2R} \text{equation 1}$$

$$(hvF) \sim (hv - E_g)^2 \text{ equation 2}$$

Where R is the reflectance, F is the Kubelka-Munk function, E_g is the bandgap and hv is the photon energy. By plotting between $(hvF)^{1/2}$ and hv , the E_g of the DCMPT, [Zn(DCMPPT)(H₂O)] and [Ag/Zn(DCMPPT)(H₂O)(OAc)] was attained.

Surface area of the [Ag-Zn(DCMPPT)(H₂O)(OAc)] complex exhibited higher than [Zn(DCMPPT)(H₂O)]. However, the ligand surface area is much lower than both the complexes and as shown in Table-2 and isotherm shown in Figure S8.

Table 2. Bandgap energies (solid phases) and Surface area of DCMPT and Zn(II)-complexes

Compound	Surface area (m ² /g)	Bandgap energy (eV) (solid-phase)
DCMPT	14	2.84
[Zn(DCMPPT)](H ₂ O)]	94	2.52
[Ag-Zn(DCMPPT)](H ₂ O)(OAc)]	156	2.42

Electrochemical studies

The redox properties of [Zn(DCMPPT)(H₂O)] and [Ag-Zn(DCMPPT)(H₂O)(OAc)] complexes are studied by applying cyclic voltammetry in CH₃CN/CHCl₃(1:1 ratio, 0.1 mol · L⁻¹ n-Bu₄NPF₆). As revealed in **Figure 8**, single-electron oxidation waves are observed in the

potential region of -2.0 to + 2.0 V (vs Ag/AgCl). This is associated with the OFL DCMPPPT, which upon coordination with a metal ion. The first oxidation potential is moved towards more negative potential, which is equally as [Zn(DCMPPT)(H₂O)]. Moreover, a change in [Ag-Zn(DCMPPT)(H₂O)(OAc)] complex is also observed [40-42], due to the Ag ions coordinated with the N of pyridine and exists between two molecules/ layers of Zn(II) complexes. This shift can be described by the electronic interactions between the DCMPPPT unit and the Zn²⁺ ions produced by the shorter distance among them [43].

Emission spectra

Emission spectra of ligand and complexes were verified in the solid phase and the materials were excited at 380 nm, 400 nm and 420 for DCMPPPT, [Zn(DCMPPT)(H₂O)] and [Ag-Zn(DCMPPT)(H₂O)(OAc)] respectively by using slit width of 5 nm. Emission spectra provided important evidence about the recombination rate of holes and electrons. From these facts, it is noticed that the efficiency of the transfer of carriers or trapping of charge to examine the probability of generation of electron-hole pair from [Ag-Zn(DCMPPT)(H₂O)(OAc)] [44]. As the emission initiates from the recombination of excited holes and electrons, greater emission strength specifies a greater rate of recombination of charge carriers and vice versa. The emission strength of [Ag-Zn(DCMPPT)(H₂O)(OAc)] was declined almost completely when related to the complex [Zn(DCMPPT)(H₂O)], as exhibited in **Figure 9**. The lower emission strength of the [Ag-Zn(DCMPPT)(H₂O)(OAc)] complex designates that a low recombination rate, which suggests that [Ag-Zn(DCMPPT)(H₂O)(OAc)] can worthily accelerate up the unraveling of electrons and holes and exhibit high photodegradation rate ability.

Photocatalysis

Photodegradation of dye pollutants

In the presence of metal complexes, photodegradation of organic dye toxins follows two methods which are i) mineralization (char) and ii) conversion of small fragments of the pollutants with stable biodegradable nature [45]. Acid violet 7 (AV7) [46], acid blue 1 (AB1) [47] and Reactive Red 120 (RR 120) [48,49] are the maximum toxic dyes usually used for the dyeing procedure in the manufacturing of clothes. B. Subash et.al., studied photodegradation of AB 1/AV 7/RR 120 dyes by using ZnO-Ag-ZnS under UV light irradiation [46], however, UV light is not suitable for industrial purpose. Hence, to overcome this drawback, here the degradation of AV 7, AB 1, and RR 120 with/without the presence of Zn(II) complexes, in absence and

presence of the visible light were examined and the outcomes are revealed in **Figure 10**. Initially, the photodegradation of AV 7, AB 1 and RR 120 dyes are carried out in dark for 20 min. After 20 min, the samples were collected and examined by UV-vis absorption spectroscopy and found that there is no considerable change in the absorption of toxins even in the occurrence of a Zn(II) complexes (hardly less than 1%). In the presence of visible light alone, the dye's photodegradation was noticed was too small (up to 1%), it is due to the lack of a photocatalyst. Later on, as soon as the Zn(II) complex was applied under visible light, the photodegradation proceeded at a controlled rate, depends on the complex applied as photocatalyst. In the presence of [Ag-Zn(DCMPPT)(H₂O)(OAc)], 80%, 65% and 74% of the concentration of respective pollutants were noticed in electronic spectra after 40 minutes, and 98 % photomineralization was also noted after 60 minutes. However, in the case of, [Zn(DCMPPT)(H₂O)], gave 50 % photodegradation after 40 min and 70 % after 60 min. Thus, [Ag-Zn(DCMPPT)(H₂O)(OAc)] is the most effective catalyst among the two complexes. The technique of degradation was also checked by mass spectrometry, the fragmented process of dye molecules was examined and presented in Table S1. After 50 min, [Ag-Zn(DCMPPT)(H₂O)(OAc)] sample was studied and it exhibited a peak at 108 m/z (Figures S9-S11). It is evident from these observed peaks that the catalyst capably causes the breaking of dye molecules in a quick duration of time. The peak is shown in mass spectra identified as benzoquinone, which is the first product of dye-pollutant photodegradation as revealed in Figure S11. Subsequently, benzoquinone peak is disappeared after 60 min, which is evident for further photomineralization. In the case of, [Zn(DCMPPT)(H₂O)], still, m/z 108 base peak (benzoquinone) was existing after 60 min of visible light (LED) illumination.

The photoreactivity of a MOF turns on several factors, such as surface area, surface structure, bandgap energy, the absorptivity of the pollutant, the geometry of the material, and rate of recombination of holes and electrons. The presence of Ag and Zn metals has a valued effect on photoreactivity because of the tridentate OFL system. The enhanced rate of photodegradation under visible light irradiation may be because of (i) the low E_g value falls into the visible light domain for [Ag-Zn(DCMPPT)(H₂O)(OAc)], (ii) Ag ions highly photosensitive in nature, which helps in the separation of hole-electron pair in the presence of visible light irradiation. [Ag-Zn(DCMPPT)(H₂O)(OAc)] complex band moved towards the higher wavelength (reduced bandgap) side due to the occurrence of Ag ions compared with [Zn(DCMPPT)(H₂O)] complex.

The Ag ions are showed dual nature as existence under visible light which is confirmed through UV-visible spectral studies and spectra revealed that i) Ag nanoparticles formed [50] on the surface ii) which boosted the photocatalytic performance of $[\text{Zn}(\text{DCMPPT})(\text{H}_2\text{O})]$ and as shown in **Figure 11**. After completion of photoreaction, visible light turned off and $[\text{Ag-Zn}(\text{DCMPPT})(\text{H}_2\text{O})(\text{OAc})]$ complex was separated and washed with acetone and dried and measured the UV-vis spectra as shown in the Figure S12. The purity and structural stability of $[\text{Ag-Zn}(\text{DCMPPT})(\text{H}_2\text{O})(\text{OAc})]$ complex verified with NMR spectra and obtained spectral data compared with pure complex (before photocatalysis) as shown in Figure S13. The NMR spectra provides an important information that after visible light turn-off, it is found the original complex re-generation. Hence, $[\text{Ag-Zn}(\text{DCMPPT})(\text{H}_2\text{O})(\text{OAc})]$ complex used for reusable and stability studies.

Further organic dye pollutants commonly used for the dying process in the manufacturing of clothes such as AB 1 and RR 120 were also studied for the degradation process with these photocatalysts. As shown in Figure 10b and 10c, analogous effects were noted, i.e., $[\text{Ag-Zn}(\text{DCMPPT})(\text{H}_2\text{O})(\text{OAc})]$ afforded a well-organized photocatalytic system for photodegradation process than $\text{Zn}(\text{DCMPPT})(\text{H}_2\text{O})$.

Degradation of industrial wastewater (sample collected from Food processing Units)

The industrial wastewater (IWW) samples are tested with LC-MS technique and data revealed a wide range of peaks with different m/z values as shown in Figure S14 & S15. From this information, some important peaks are identified and matched with pesticide molecular weight and the rest of the peaks are unknown pollutants that were formed through the food processing methods. After initial analysis, the IWW samples are exposed to visible light irradiation in the presence of $[\text{Ag-Zn}(\text{DCMPPT})(\text{H}_2\text{O})(\text{OAc})]$ photocatalyst. Then, the tested sample solutions are taken with regular time intervals and measured the concentration of the sample by UV-visible spectra. The data revealed that the concentration of pollutants was gradually decreased and finally, after 240 minutes completely degraded the pesticides and unknown pollutants present in the IWW samples as shown in **Figure 12**. The sample solution was remeasured with LC-MS maximum peaks are disappeared as compared with initial data (Figure S12). Therefore, $[\text{Ag-Zn}(\text{DCMPPT})(\text{H}_2\text{O})(\text{OAc})]$ complex performance towards the photocatalytic degradation of IWW is higher than $[\text{Zn}(\text{DCMMPT})(\text{H}_2\text{O})]$ complex. Lastly, the photodegraded IWW attained was examined for chemical oxygen demand (COD) experiment

with $K_2Cr_2O_7$ as the oxidizing agent. The COD value recorded for photo-mineralized wastewater sample is 205 mg/L, as compared with 992 mg/L for the initial IWW sample. With a typical value of 250 mg/L, the photo-mineralization of contaminants existing in TPE generated water can be reusable [5].

Kinetic Studies

Moreover, as revealed in **Figure S16**, the reaction kinetics plots mechanically reveal the catalytic efficiency modifications under the two photocatalysts enlightened above. Subsequently, the photomineralization performance of AV 1 dye solution follows the first-order reaction, the reaction kinetic plot was deduced from the formulae between $\ln(C/C_0)$ and time (t)

$$\ln(C/C_0) = -kt \quad (1)$$

The rate constant k of photocatalysis with $[Zn(DCMMPT)(H_2O)]$ and $[Ag-Zn(DCMPPT)(H_2O)(OAc)]$ complexes were 0.04205, and 0.14098 min^{-1} respectively. The k value of $[Ag-Zn(DCMPPT)(H_2O)(OAc)]$ complex photocatalysis process was 3.35 times faster than simple $[Zn(DCMMPT)(H_2O)]$ complex.

Identification of active species

Generally, the photodegradation reaction depends on four kinds of active species like superoxide radical ($O_2^{\bullet-}$), electron (e^-), hole (h^+) and hydroxyl radical ($\bullet OH$) [51-54] in the existence of photocatalyst. In order to identify the active species involved in photodegradation of dye pollutants, few types of foragers (t-butanol, benzoquinone, EDTA and $K_2S_2O_8$, same quantity with respective photocatalyst) used in the photodegradation process. As revealed in **Figure 13**, photodegradation of AV 7 over $[Ag-Zn(DCMPPT)(H_2O)(OAc)]$ was delayed with the occurrence of t-butanol (TBA), benzoquinone (BQ), ethylene diamine tetra acetic acid (EDTA) and potassium peroxydisulphate ($K_2S_2O_8$). The outcomes specified that hydroxy radicals ($\bullet OH$), and holes are the highly active species involved in the photomineralization of AV 7. However, $\bullet OH$ was more dominant in photomineralization of AV 7 as compared to hole species. In presence of TBS and $K_2S_2O_8$ are responsible for the reducing in the mineralization of AV 7 due to the presence of $\bullet OH$ and hole scavengers (figure 14). The presence of BQ had very less effect on the mineralization rate, signifying that AV 7 was almost not degraded by $O_2^{\bullet-}$. Therefore, the entire photodegradation reactions depend on the $\bullet OH$ and hole scavengers, which are the most important species for photomineralization.

Reusable studies of the photocatalyst

The stability and reusability of photocatalyst are examined, by using catalyst separated from tested solution through the centrifuged method. It was noticed that the photocatalyst sustained as same dark gray color, signifying that organic dye pollutants were not deposited on the surface of the photocatalyst and the total pollutants are photomineralized, which is confirmed from elemental analysis of the complex as matched with pure complex data. Continuous reuse of bimetallic complex after four runs of photodegradation of organic dye pollutants, the [Ag-Zn(DCMPPT)(H₂O)(OAc)] complex was separated and recorded ¹H-NMR spectra. From the spectra it is confirmed that the bimetallic complex is stable up to four cycles (shown Figure S13). However, after fifth cycle ¹H-NMR spectral data shows mixture of both the complexes such as [Zn(DCMPPT)(H₂O)] and [Ag-Zn(DCMPPT)(H₂O)(OAc)] in the ratio of 15:85 as represented in **Figure S17**, which indicates that [Ag-Zn(DCMPPT)(H₂O)(OAc)] complex stability is decreased after four runs of photodegradation of organic pollutants. As shown in **Figure 14**, the performance of the photocatalysts is with not much changes in photodegradation of pollutants after sequential turns (four cycles).

The performance of the catalyst slowly declines due to Ag ions are converted into Ag₂O [55,56] and separated from [Zn(DCMPPT)(H₂O)] which is further characterized by powder XRD (the PXRD pattern based on the POWD computed software) and shown in **Figure 15**. The photodegradation was carried out for five runs (60 min. each) and the yields are 97, 95, 94, 93 and 90% (the gradual decrease in the yields for five continuous runs are due to formation of Ag₂O, shown in figure 16), which shows the reusability of catalyst. The results reveal that the photocatalytic activity of [Ag-Zn(DCMPPT)(H₂O)(OAc)] could be repeated without a substantial drop in the catalyst efficiency.

Conclusion

Zn((E)-3-(((4,5-dichloro-2-mercaptophenyl)imino)methyl)pyridine-2-thiol)(H₂O) and [Ag-Zn((E)-3-(((4,5-dichloro-2-mercaptophenyl)imino)methyl)pyridine-2-thiol)(H₂O)(OAc)] were synthesized and confirmed through various spectroscopic methods. The dual nature of Ag ions under visible light was confirmed by UV-visible spectra. The catalytic property of new Zn (II) based complexes for various organic dye pollutants was studied under visible-light-driven. The photocatalytic performance of [Ag-Zn(DCMPPT)(H₂O)(OAc)] complex is greater than [Zn(DCMPPT)(H₂O)] complex and is highly stable even after five cycles. Moreover, photodegradation investigations proposed that the bimetallic complex with better photocatalytic

performance will be a possible candidate for reusable wastewatercleansingunder visible-light-driven.

Credit author statement

Methodology, Investigation, Formal analysis and Writing – original draft by Mahesh Subburu.

Photochemical reactions performance by Ramesh Gade.

Characterization of Mass spectral data by Venkanna Guguloth.

Koteshwar Rao Ravulapelly provide Thermogravimetric and XPS analysis of complexes

UV-visible DRS and PL spectral data provided by Dr. Prabhakar Chetti.

Conceptualization, Validation, Formal analysis, Resources, Writing – review and editing, Supervision and Project administration by Dr. Someshwar Pola.

Someshwar Pola

Conflict of Interest and Authorship Conformation Form

Please check the following as appropriate:

- All authors have participated in (a) conception and design, or analysis and interpretation of the data; (b) drafting the article or revising it critically for important intellectual content; and (c) approval of the final version.
- This manuscript has not been submitted to, nor is under review at, another journal or other publishing venue.
- The authors have no affiliation with any organization with a direct or indirect financial interest in the subject matter discussed in the manuscript
- The following authors have affiliations with organizations with direct or indirect financial interest in the subject matter discussed in the manuscript:

Author's name	Affiliation
Mahesh Subburu	Osmania University
Ramesh Gade	Osmania University
Venkanna Guguloth	Osmania University
Koteshwar Rao Ravelapelly	Osmania University
Prabhakar Chetti	NIT, Kurukshetra, India
Someshwar Pola	Osmania University

Acknowledgment

Authors would like to thank DST - FIST schemes and UGC, New Delhi. Mahesh Subburu thanks University Grants Commission (UGC), New Delhi for the award of Junior Research Fellowship and SP for financial support under SERB (EMR//2014/000452), UGC-UPE-FAR and DST-PURSE, New Delhi, India.

References

- [1] E. Brillas, I. Sirés, M. A. Oturan, Chem. Rev., 109(2009) 6570-6631.
- [2] H. Hassan, S. Dai, B. Jin, ACS Sus. Chem. & Eng., 7(2019) 17263-17272.
- [3] P. Avetta, F. Bella, A. B. Prevot, E. Laurenti, E. Montoneri, A. Arques, L. Carlos, ACS Sus. Chem. & Eng., 1(2013) 1545-1550.
- [4] X. Zou, J. Liu, J. Su, F. Zuo, J. Chen, P. Feng, Chem. Eur. J. 19 (2013) 2866-2873.
- [5] R. Gade, J. Ahemed, K. L. Yanapu, S. Y. Abate, Y. -T. Tao, S. Pola, J. Environ. Chem. Eng., 6 (2018) 4504-4513.
- [6] A. Karci, Chemosphere, 99 (2014) 1-18.
- [7] J. Lee, U. von Gunten, J. -H. Kim, Environ. Sci. & Tech., 54(2020) 3064-3081.

- [8] Z.-Z. Yang, C. Zhang, G.-M. Zeng, X. -F. Tan, H. Wang, D. -L. Huang, K. -H. Yang, J.-J. Wei, C. Ma, K.Nie, *J. Mater. Chem. A*, 8 (2020) 4141-4173.
- [9] M. L. Pegis, C. F. Wise, D. J. Martin, J. M. Mayer, *Chem. Rev.*, 118 (2018) 2340-2391.
- [10] K. P. Bryliakov, *Chem. Rev.*, 117 (2017) 11406-11459.
- [11] X. Liu, Y. Zhou, J. Zhang, L. Tang, L. Luo, G. Zeng, *ACS Appl. Mater. Inter.*, 9(2017) 20255-20275.
- [12] J. M. L. Martinez, M. F. L. Denis, L. L. Piehl, E. R. de Celis, G. Y. Buldain, V. C. D. Orto, *Appl. Catal. B*, 82 (2008) 273–283.
- [13] X. -L. Yan, D. -Y. Ma, *Inorg. Chem. Commun.*, 104 (2019) 31-35.
- [14] S. A. A. Razavi, A. Morsali, *Coord. Chem. Rev.*, 399 (2019) 213023.
- [15] S. Gazi, R. A. Krishnan, N. D. P. Singh, *J. Hazard. Mater.*, 183 (2010) 894–901.
- [16] N.B. G. Reddy, P. M. Krishna, N. Kottam, *Spectrochim. Acta A*, 137 (2015) 371–377.
- [17] H. -H. Wang, J. Yang, Y. -Y. Liu, S. Song, J. -F. Ma, *Cryst. Grow. Des.*, 15(2015) 4986-4992.
- [18] S. Pola, M. Subburu, R. Guja, V. Muga, Y.-T. Tao, *RSC Adv.*, 5 (2015) 58504–58513.
- [19] V. Guguloth, J. Ahemed, M. Subburu, V. C. Guguloth, P. Chetti, S. Pola, *J. Photochem. & Photobiol. A: Chem.*, 382 (2019) 111975.
- [20] J.M. Li, X.G. Meng, C.W. Hu, J. Du, X.C. Zeng, *J. Mol. Catal. A* 299 (2009) 102–107.
- [21] S. Gazi, R.A. Krishnan, N.D.P. Singh, *J. Hazard. Mater.* 183 (2010) 894–901.
- [22] B. Agboola, K. Ozoemena, T. Nyokong, *J. Mol. Catal. A: Chem.* 227 (2005) 209–216.
- [23] G.R. Reddy, S. Balasubramanian, K. Chennakesavulu, *J. Mater. Chem. A*, 2 (2014) 15598–15610.
- [24] L. F. Lindoy, *Q. Rev. Chem. Soc.*, 25 (1971) 379-391
- [25] Q. Li, Z.-L. Fan, D.-X. Xue, Y. -F. Zhang, Z. -H. Zhang, Q. Wang, H. -M. Sun, Z. Gao, J. Bai, *J. Mater. Chem. A*, 6 (2018) 2148-2156.
- [26] D. G. Musaev, T. M. Figg, A. L. Kaledin, *Chem. Soc. Rev.*, 43 (2014) 5009-5031.
- [27] W. J. Geary, *Coord. Chem. Rev.*, 7 (1971) 81–122.
- [28] T. Majumder, S. Dhar, K. Debnath, S. P. Mondal, *Mater. Res. Bull.*, 93 (2017) 214-222.
- [29] A.H. Chughtai, N. Ahmad, H.A. Younus, A. Laypkov, F. Verpoort, *Chem. Soc. Rev.*, 44 (2015) 6804–6849.
- [30] P. Sharma, A.P. Singh, *RSC Adv.* 4 (2014) 43070–43079.

- [31] M. Azam, Z. Hussain, I. Warad, S.I. Al-Resayes, Md.S. Khan, M. Shakir, A.T. Kruszynska, R. Kruszynski, Dalton Trans. 41 (2012) 10854–10864.
- [32] B.E. Warren, X-ray Diffraction, second ed., Dover, New York, 1990.
- [33] R. Gundeboina, N. K. Veldurthi, R. Velchuri, R. Guje, S. Pola, V. Muga, 12 (2015) 700–710.
- [34] B. R. Kumar, N. V. Prasad, G. Prasad, G. S. Kumar, Materials Today: Proceedings, 11 (2019) 1036–1040.
- [35] K. Auromun, R. N. P. Choudhary, Ceramics International, 45 (2019) 20762–20773.
- [36] S. Halder, S. Bhuyan, R. N. P. Choudhary, Eng. Sci. & Tech. Inter. J., 22 (2019) 376–384.
- [37] S.J. Swamy, S. Pola, Spectrochim. Acta A 70 (2008) 929–933.
- [38] A. Bocian, D. Brykczyńska, M. Kubicki, Z. Hnatejko, M. W. -Chorab, A. Gorczyński, V. Patroniak, Polyhedron, 157 (2019) 249–261.
- [39] C.A.D. Amato, R. Giovannetti, M. Zannotti, E. Rommozzi, S. Ferraro, C. Seghetti, M. Minicucci, R. Gunnella, A. Di Cicco, Appl. Surf. Sci. 441 (2018) 575–587.
- [40] A. Juris, V. Balzani, F. Barigelletti, S. Campagna, P. Belser, A. von Zelewsky, Coord. Chem. Rev. 84 (1988) 85–277.
- [41] J. Qin, S.Y. Deng, C.X. Qian, T.Y. Li, H.X. Ju, J.L. Zuo, J. Organomet. Chem. 750 (2014) 7–12.
- [42] J. Qin, L. Hu, N. Lei, Y.-F. Liu, K.-K. Zhang, J.-L. Zuo, Acta Chim. Slov. 61 (2014) 740–745.
- [43] L. Hu, W. Liu, C.H. Li, X.H. Zhou, J.L. Zuo, Eur. J. Inorg. Chem. 35 (2013) 6037–6048.
- [44] N. Yoshinari, T. Shimizu, K. Nozaki, T. Konno, Inorg. Chem. 55 (2016) 2030–2036.
- [45] L. Li, P.A. Salvador, G.S. Rohrer, Nanoscale 6 (2014) 24–42.
- [46] B. Subash, B. K. Kumar, M. Swaminathan, M. Shanthi, Ind. Eng. Chem. Res., 53 (2014) 12953–12963.
- [47] C. -C. Chen, H. -J. Fan, J. -L. Jan, J. Phys. Chem. C, 112 (2008) 11962–11972.
- [48] J. Paul, K. P. Rawat, K. S. S. Sarma, S. Sabharwal, Appl. Rad. & Iso., 69 (2011) 982–987.
- [49] V. Kumar, S. Mandar, P. Badve, A. B. Pandit, Chem. Eng. J., 178 (2011) 100–107.
- [50] D. K. Bhui, H. Bar, P. Sarkar, G. P. Sahoo, S. P. De, A. Misra, J. Mol. Liq., 145 (2009) 33–37.
- [51] J.-D. Xiao, H.-L. Jiang, Acc. Chem. Res. 52 (2019) 356–366.

- [52] N. Chumha, W. Pudkon, A. Chachvalvutikul, T. Luangwanta, C. Randorn, B. Inceesungvorn, A. Ngamjarrojana, S. Kaowphong, *Mater. Res. Express*, 7 (2020) 015074.
- [53] J. Sun, X. Yan, K. Lv, S. Sun, K. Deng, D. Du, *J. Mol. Catal. A: Chem.*, 367 (2013) 31-37.
- [54] J. Yao, R. Qu, X. Wang, V. K. Sharma, A. Shad, A. A. Dar, Z. Wang, *Water Res.*, 169 (2020) 115273.
- [55] Y. Zhang, Z. Chen, S. Liu, Y.-J. Xu, *Appl. Catal. B Environ.* 140–141 (2013)598–607.
- [56] T.Xaba, M.J. Moloto, M. Al-Shakban, Md.A. Malik, P. O'Brien, N. Moloto, *Mater.Sci. Semicond. Process* 71 (2017) 109–115.

Fig. 1 EDX images of a) $[\text{Zn}(\text{DCMPPT})(\text{H}_2\text{O})]$ and b) $[\text{Ag}/\text{Zn}(\text{DCMPPT})(\text{H}_2\text{O})(\text{OAc})]$ complexes.

Fig. 2 FESEM metaphors of a) DCMPPT, b) $[\text{Zn}(\text{DCMPPT})(\text{H}_2\text{O})]$ and c) $[\text{Ag}-\text{Zn}(\text{DCMPPT})(\text{H}_2\text{O})(\text{OAc})]$.

Fig. 3 Thermograms of $[\text{Zn}(\text{DCMPPT})(\text{H}_2\text{O})]$ and $[\text{Ag}/\text{Zn}(\text{DCMPPT})(\text{H}_2\text{O})(\text{OAc})]$ complexes.

Fig. 4 XPS spectra of a) $[\text{Zn}(\text{DCMPPT})(\text{H}_2\text{O})]$ and b) $[\text{Ag}/\text{Zn}(\text{DCMPPT})(\text{H}_2\text{O})(\text{OAc})]$ complexes

Fig. 5 Powder XRD pattern of ligand and complexes.

Fig. 6 Tentative structures of $[\text{Zn}(\text{DCMPPT})(\text{H}_2\text{O})]$ and $[\text{Ag}-\text{Zn}(\text{DCMPPT})(\text{H}_2\text{O})(\text{OAc})]$ complexes.

Fig. 7 a) UV-vis and b) UV-vis-DRS spectra of ligand and complexes.

Fig. 8 Cyclic voltograms of ligand and complexes.

Fig. 9 PL spectra of ligand and complexes.

Fig. 10 Photodegradation of a) AV 7, b) AB 1, and c) RR 120 with $[\text{Zn}(\text{DCMPPT})(\text{H}_2\text{O})]$ and $[\text{Ag}-\text{Zn}(\text{DCMPPT})(\text{H}_2\text{O})(\text{OAc})]$ and d), e) and f) successive absorbance spectral patterns of AV 7, AB 1 and RR 120 with $[\text{Ag}-\text{Zn}(\text{DCMPPT})(\text{H}_2\text{O})(\text{OAc})]$.

Fig. 11 UV-visible spectra of in-situ formed Ag NPs.

Fig. 12 a) Photodegradation of IWW in the presence of $[\text{Ag}-\text{Zn}(\text{DCMPPT})(\text{H}_2\text{O})(\text{OAc})]$ b) successive absorbance spectral pattern and c) box chart plot for % of dye degradation under visible-light-driven.

Fig. 13 Control tests of selective photodegradation of AV 7 with the adding of several radical foragers: tert-butyl alcohol (TBA, scavenger for hydroxyl radicals), benzoquinone (BQ, forager

for superoxide radicals), K₂S₂O₈ (KSO scavenger for electrons) and Ethylenediaminetetraacetic acid (EDTA, scavenger for holes) over the optimum [Ag-Zn(DCMPPT)(H₂O)(OAc)] under visible light irradiation.

Fig. 14 Performance of [Ag-Zn(DCMPPT)(H₂O)(OAc)] complex upon reusable with 5 cycles of degradation process of AB 1, AV 7 and RR 120 dyes.

Fig. 15 Powder XRD image of [Ag-Zn(DCMPPT)(H₂O)(OAc)] photocatalyst after 5 cycles of degradation of AV 7 dye.

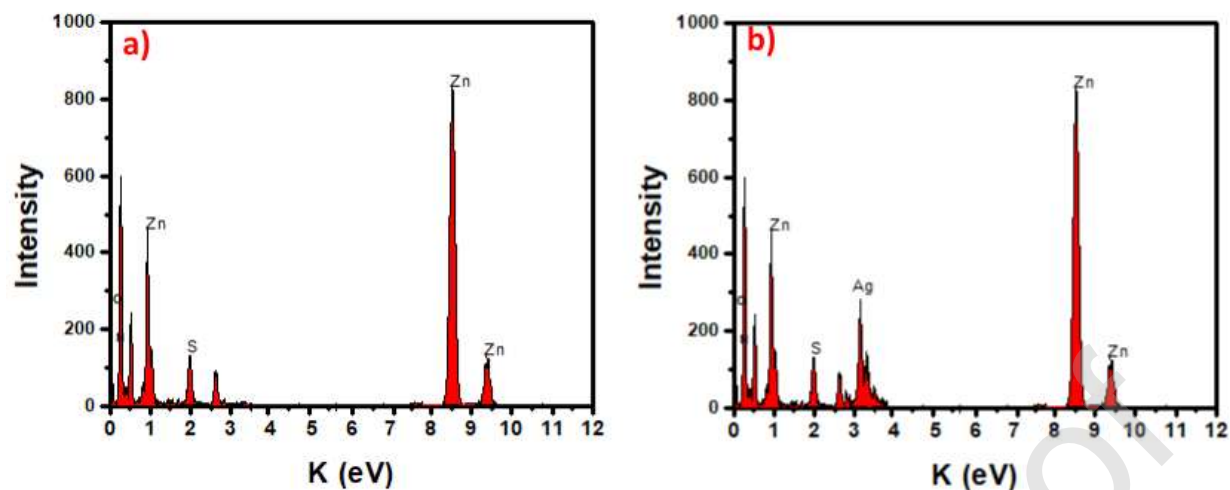


Fig. 1 EDX images of a) $[\text{Zn}(\text{DCMPPT})(\text{H}_2\text{O})]$ and b) $[\text{Ag}/\text{Zn}(\text{DCMPPT})(\text{H}_2\text{O})(\text{OAc})]$ complexes

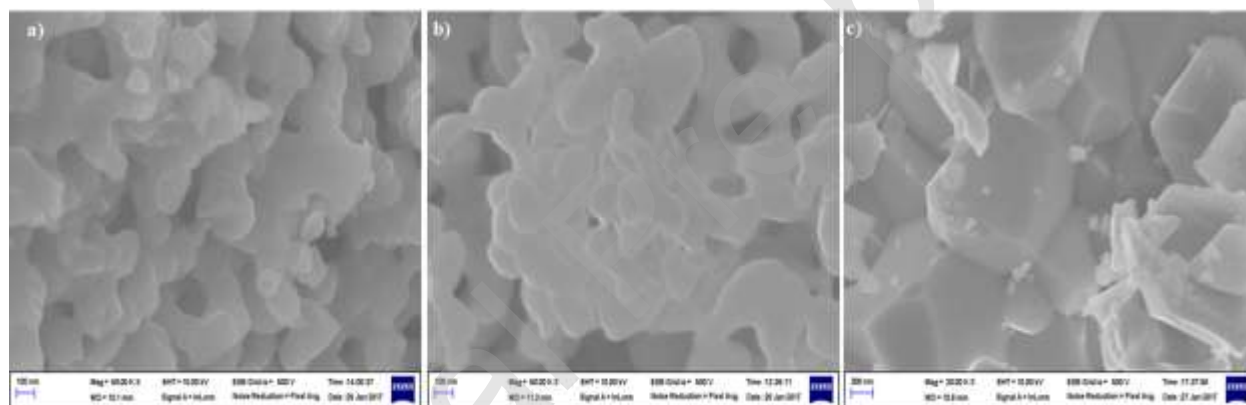


Fig. 2 FESEM metaphors of a) DCMPTT, b) $[\text{Zn}(\text{DCMPPT})(\text{H}_2\text{O})]$ and c) $[\text{Ag}/\text{Zn}(\text{DCMPPT})(\text{H}_2\text{O})(\text{OAc})]$

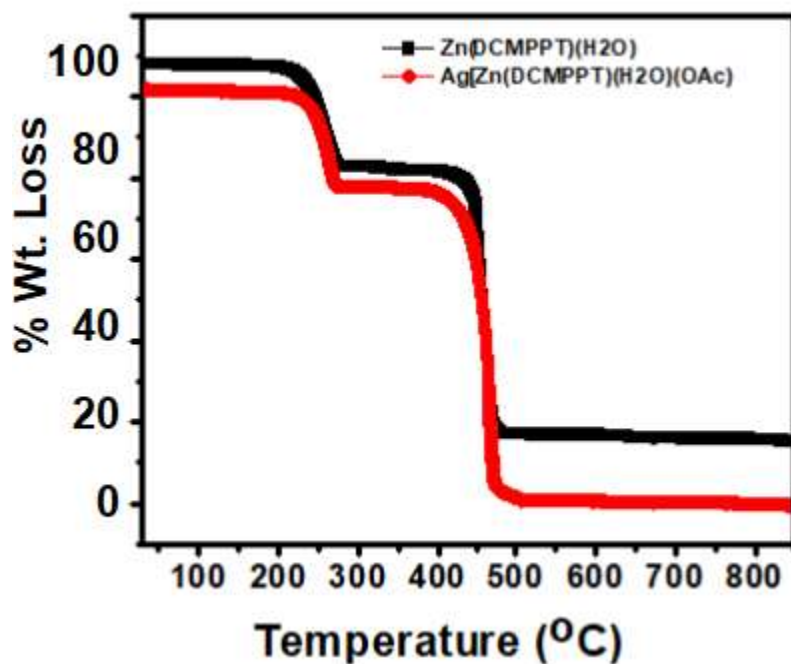


Fig. 3 Thermograms of both the complexes

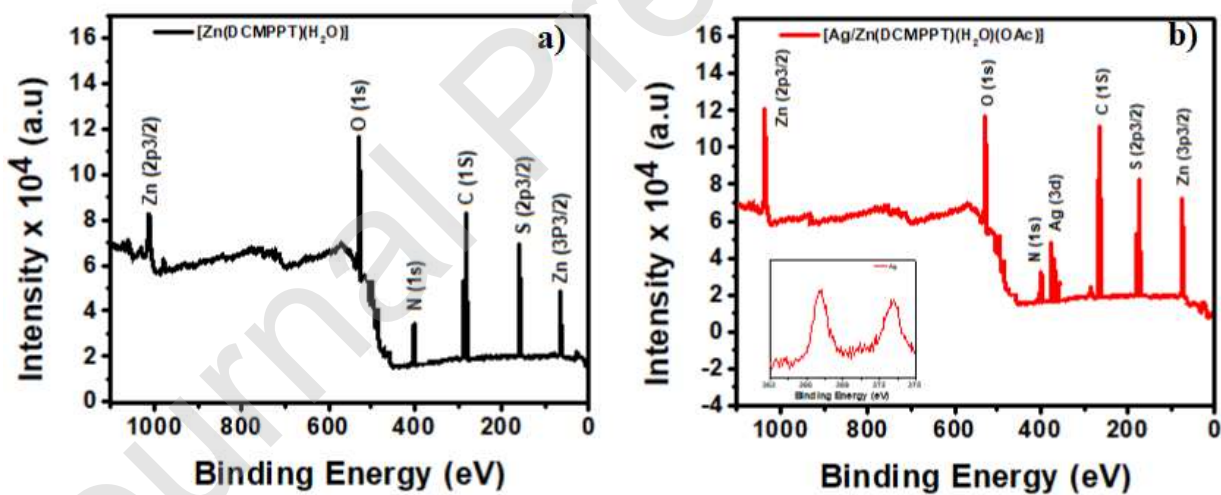


Fig. 4 XPS spectra of a) [Zn(DCMPPT)(H₂O)] and b) [Ag/Zn(DCMPPT)(H₂O)(OAc)] complexes

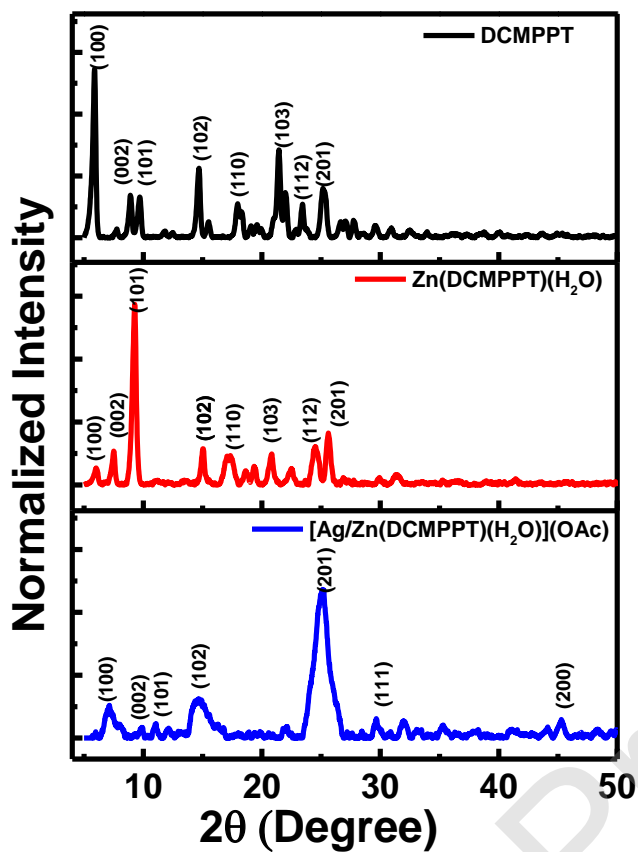


Fig. 5 powder XRD pattern of ligand and complexes

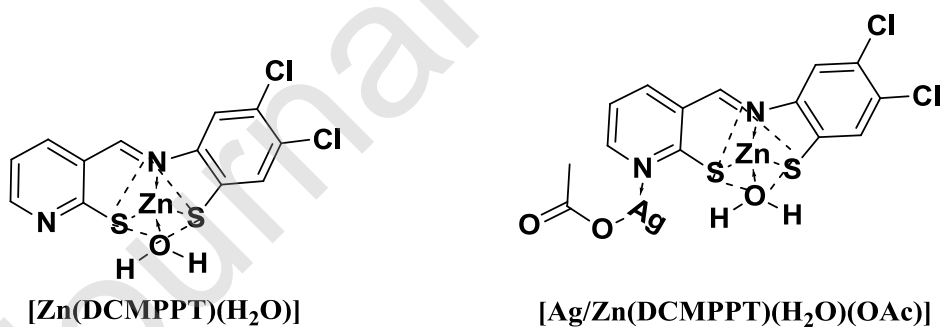


Fig.6 Tentative structures of $[Zn(DCMPPT)(H_2O)]$ and $[Ag-Zn(DCMPPT)(H_2O)(OAc)]$ complexes

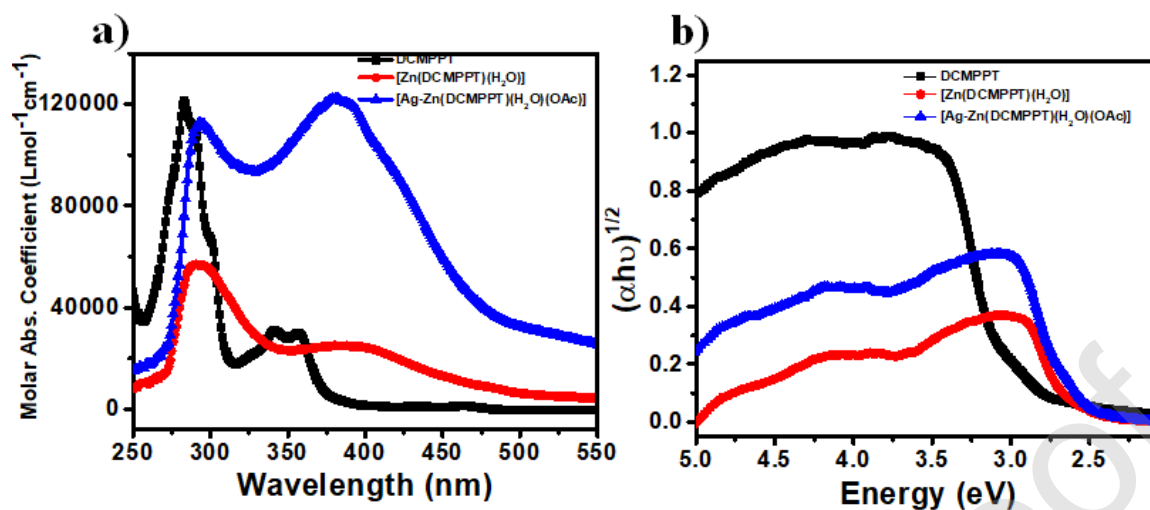


Fig. 7 a) UV-vis and b) UV-vis-DRS spectra of ligand and complexes

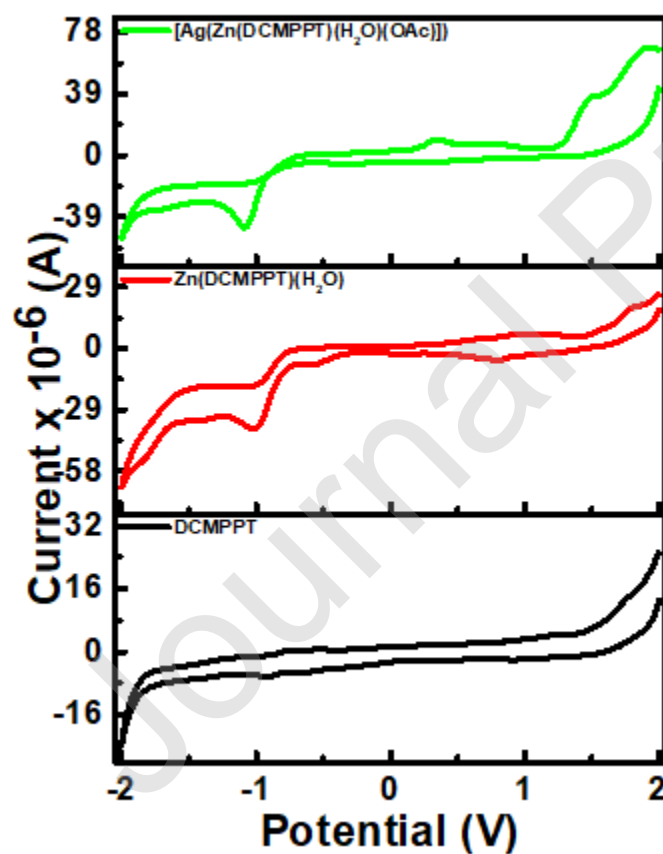


Fig. 8 Cyclic voltammograms of ligand and complexes

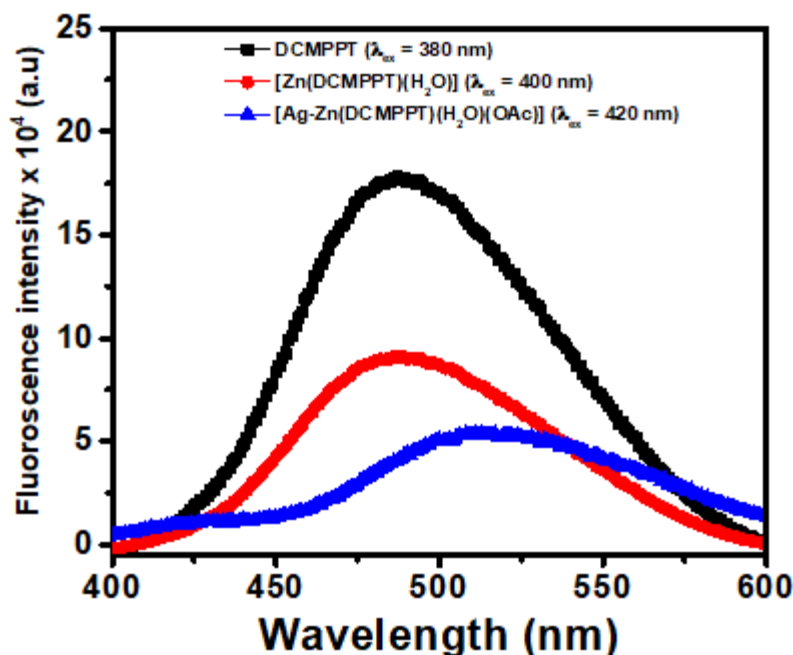


Fig. 9 PL spectra of ligand and complexes

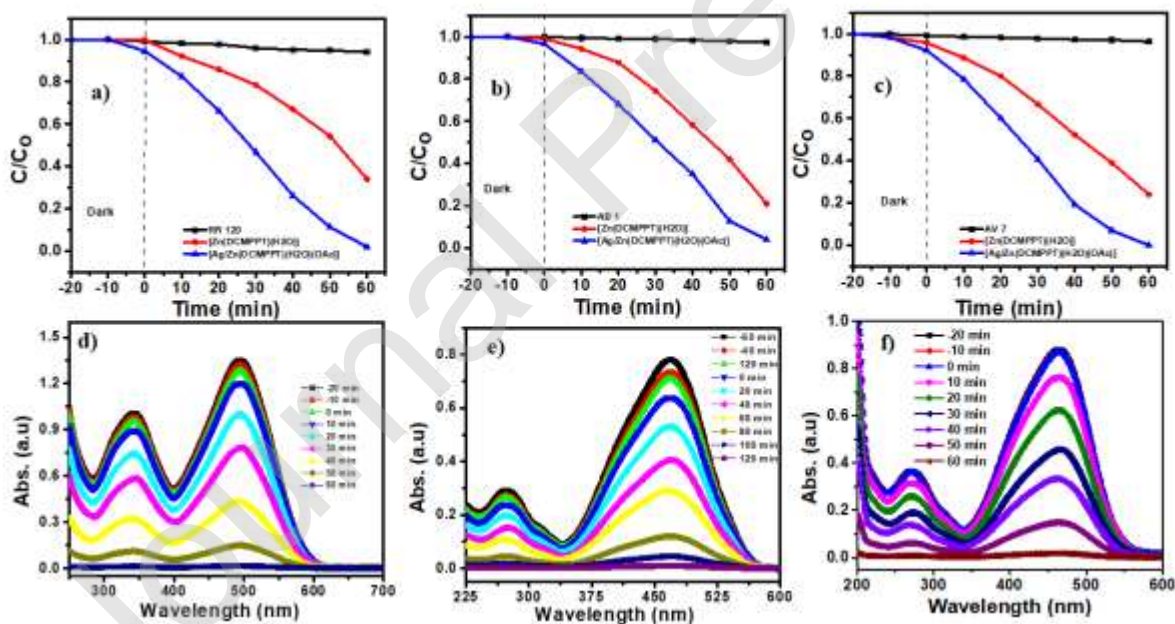


Fig. 10 Photodegradation of a) AV 7, b) AB 1, and c) RR 120 with $[Zn(DCMPPT)(H_2O)]$ and $[Ag-Zn(DCMPPT)(H_2O)(OAc)]$ and d), e) and f) successive absorbance spectral patterns of AV 7, AB 1 and RR 120 with $[Ag-Zn(DCMPPT)(H_2O)(OAc)]$.

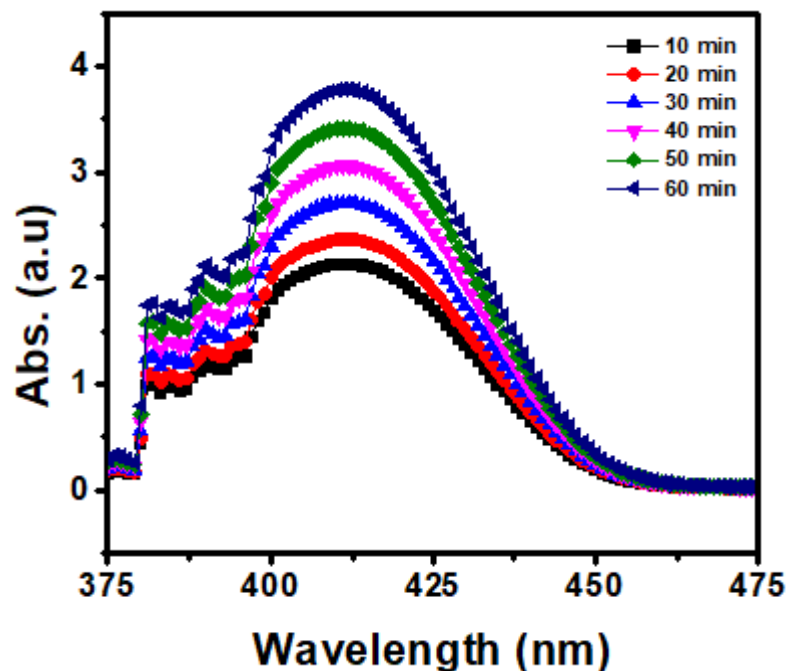


Fig. 11 UV-visible spectra of in-situ formed Ag NPs.

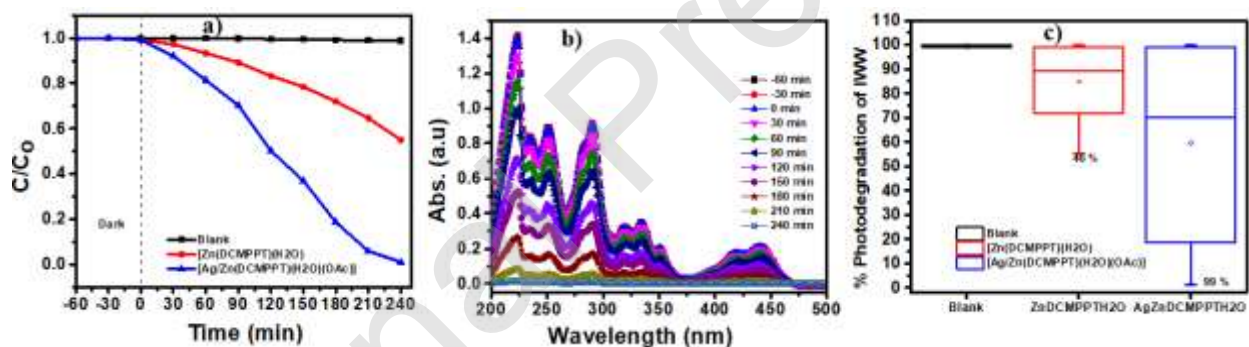


Fig. 12 a) Photodegradation of IWW in the presence of $[Ag-Zn(DCMPPT)(H_2O)(OAc)]$ b) successive absorbance spectral pattern and c) box chart plot for % of dye degradation under visible-light-driven.

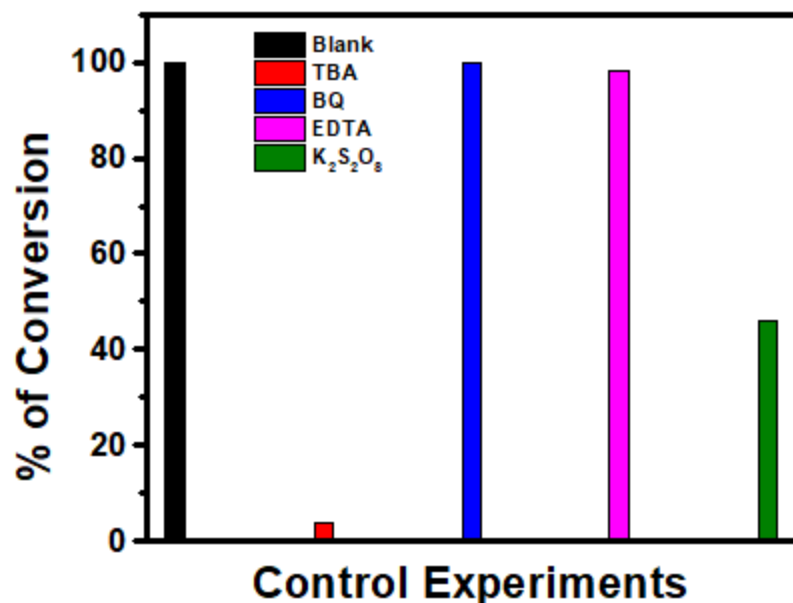


Fig. 13 Control tests of selective photodegradation of AV 7 with the adding of several radical foragers: tert-butyl alcohol (TBA, scavenger for hydroxyl radicals), benzoquinone (BQ, forager for superoxide radicals), K₂S₂O₈ (KSO scavenger for electrons) and Ethylenediaminetetraacetic acid (EDTA, scavenger for holes) over the optimum [Ag-Zn(DCMPPT)(H₂O)(OAc)] under visible light irradiation.

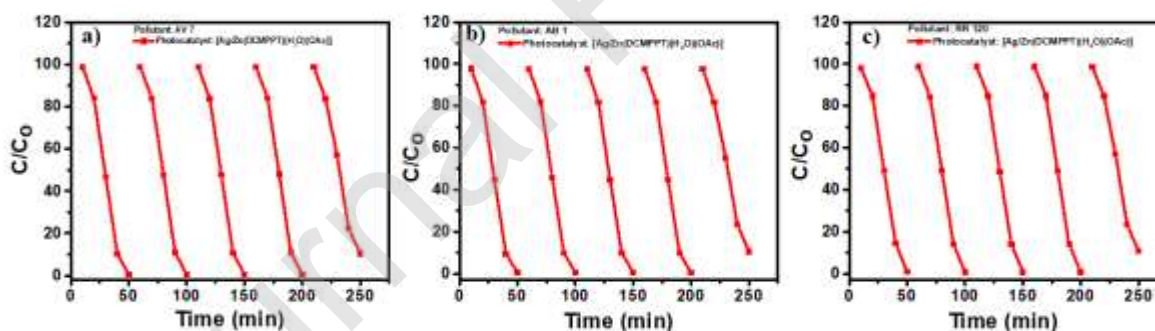


Fig. 14 Performance of [Ag-Zn(DCMPPT)(H₂O)(OAc)] complex upon reusable with 5 cycles of degradation process of AB 1, AV 7 and RR 120 dyes.

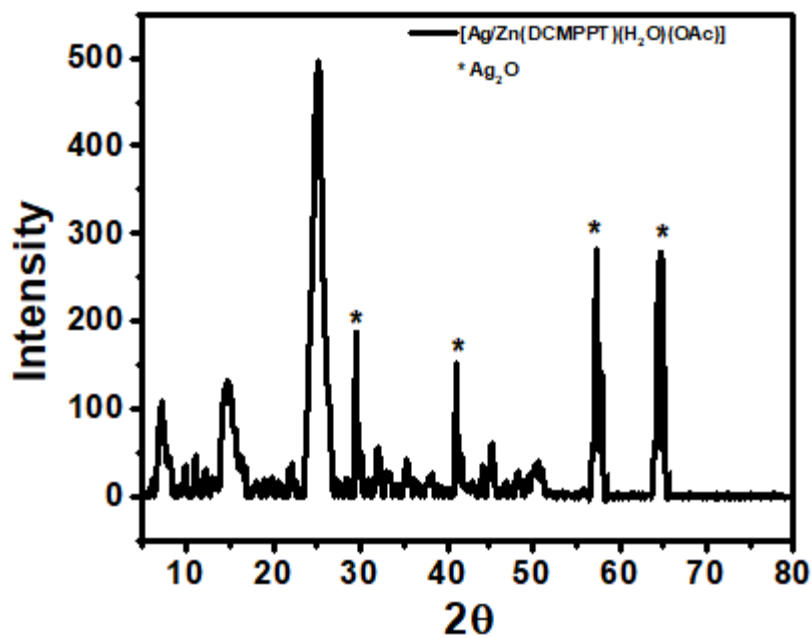


Fig. 15 Powder XRD image of [Ag-Zn(DCMPPT)(H₂O)(OAc)] photocatalyst after 5 cycles of degradation of AV 7 dye.